Desalination and Water Treatment
www.deswater.com

doi: 10.5004/dwt.2019.23911

155 (2019) 175–182
July

Removal of trace Cs(I), Sr(II), and Co(II) in aqueous solutions using continuous electrodeionization (CEDI)

Bei Jiang[a], Fuzhi Li[a], Xuan Zhao[a,b,*]

[a]*Collaborative Innovation Center for Advanced Nuclear Energy Technology, Institute of Nuclear and New Energy Technology (INET), Tsinghua University, Beijing 100084, China, emails: zhxinet@tsinghua.edu.cn (X. Zhao), jiangbei187@163.com (B. Jiang), li-fz@tsinghua.edu.cn (F. Li)*
[b]*Beijing Key Laboratory of Radioactive Wastes Treatment, Tsinghua University, Beijing 100084, China*

Received 9 September 2018; Accepted 3 February 2019

ABSTRACT

Nuclear power plants produce low-level radioactive wastewaters (LLRW) that contain radioactive nuclides. Prior to discharge, these radioactive nuclides need to be safely and efficiently removed. Continuous electrodeionization (CEDI) has shown potential for the treatment of LLRW. Here, we measured the performance of CEDI stacks on the removal of three different trace nuclides: Cs(I), Sr(II) and Co(II). Our results indicated that Cs(I) and Sr(II) actively migrated in the resin particles and were distributed in the resin profile according to the applied electric field. Nuclide removal was improved by increasing the working current. At a working current of 0.5 A, the removal efficiencies of Cs(I), Sr(II), and Co(II) amounted to 99.7%, 98.1%, and 77.1%, respectively. However, excessive working current resulted in the hydrolysis and formation of $Co(OH)_2$ which deposited on the surface of the cation exchange resin. The adsorption rate of Cs(I), Sr(II), and Co(II) for the resin was in the following order: Cs(I) > Sr(II) > Co(II). This order was also positively related to the removal efficiency of the CEDI stack. However, we found no significant relationship between resin adsorption capacity and CEDI removal efficiency.

Keywords: Continuous electrodeionization; Nuclides; Ion transport; Wastewater

1. Introduction

As it is a clean energy, nuclear power has great development potential in China. To this end, the 13th Five-Year Plan included a 2020 milestone: China will achieve 58 GW of operating, nuclear power capacity and have under construction an additional 30 GW of nuclear power capacity. When these nuclear power plants are in operation, a large amount of low level radioactive wastewaters (LLRW) will be generated mostly from their primary coolant. Fission products and corrosion products are the main source of radionuclides in primary coolants, like Sr(II), Cs(I) and Co(II). There are almost no other non-radioactive salt ions [1]. The radioactive waste will destroy the natural ecosystems and threaten the human health, high dose irradiation can lead to human chromosome aberration and gene mutation. So it has to be purified before being discharged into the environment [2].

At present, there are many new researches on the removal of radionuclides from wastewater [3,4]. Continuous electrodeionization (CEDI) is a hybrid water treatment technology that is suitable for the treatment of low salinity wastewater. It also has a high decontamination factor [5,6]. CEDI has been recognized as a potential technology for the removal of trace nuclides and as a way to minimize radioactive waste [7,8]. The CEDI stack has both dilute and concentrated compartments, which are alternately arranged between electrodes and separated by an

* Corresponding author.

ion-exchange membrane. Compared with ED, ion exchange resins are packaged into the compartments to improve the electrical conductivity of the stack. With an applied working current, the ions in the dilute compartment will migrate directly to the concentrated compartment [9,10].

The conventional technologies for handling LLRW are evaporation and ion exchange, mainly because of their historic use, efficiency, and simplicity [11]. However, evaporation suffers from several well-known problems, including energy consumption, effective scaling to large industrial levels, and corrosion [12]. Moreover, ion-exchange technology produces a large volume of radioactive, exhaust resins due to the regeneration absence in nuclear industry [13]. Compared with the conventional ion exchange process, which is widely used in NPP, CEDI can offer the favorable efficiency and simplicity. In addition, there is no accumulation of nuclides, the module can be operated continuously without exhausted resin produced in theory. Therefore, the application of CEDI can avoid the large amount of radioactive exhausted resin, which is inevitably generated in conventional ion exchange process.

According to recent reports, CEDI has been primarily used for the removal of weak acids such as $B(OH)_4^-$ [14] and heavy metals such as Ni^{2+} [15,16], Cr^{6+} [17], and Cu^{2+} [18]. It also produces highly pure water [9]. Past works by Song [19] and Zhang [20] studied the treatment of low radioactive wastewater containing Co (II) and Cs (I), respectively, using CEDI systems. Their collective results showed that CEDI was an efficient technique for the purification of nuclide-containing wastewater. Importantly, the removal ratio under optimal conditions reached up to 99%.

The study presented here was based on past investigations into the different nuclide removal efficiencies of CEDI; we then further explored the effects of the isothermic and kinetic parameters of packaged polymers in the CEDI stack.

2. Materials and methods

2.1. Materials and installation

2.1.1. Ion exchange resin

Both the strong basic anion exchange resin (AER) and strong acid cation exchange resin (CER) were purchased from Dow Chemical (Shanghai, China). They were both gels and were used in the primary system. Additional resin properties are listed in Table 1. Before packed into the CEDI stack, the resin were cleaned in the deionized water and placed in the drying oven until the resin is dried. The CER and AER were mixed in a 1:1 wet volume ratio before each experiment.

2.1.2. Ion exchange membrane

Commercial heterogeneous anion and cation exchange membranes were purchased from Qianqiu Environmental Water Treatment Co. Ltd. (Zhejiang, China). The cation and anion exchange membranes contained $–SO_3H$ and $–[N(CH_3)_3]OH$, respectively. Membranes were immersed in deionized water for more than 24 h before use to remove any soluble impurities.

2.1.3. CEDI set-up

The experiments were carried by a lab scale CEDI system, detailed in Fig. 1. Briefly, the CEDI stack had three main compartments: Two concentrate compartments and one dilute compartment, which were separated by both the cation exchange membrane (CEM) and anion exchange membrane (AEM). The effective membrane area was 44.2 cm^2. The depth of the dilute and concentrate compartments were 1 cm and 0.5 cm, respectively. The dilute compartment was packed with mixed resin in a 1:1 ratio (AER: CER = 1:1). The anode compartment was packed with AER and cathode compartment was packed with CER. The cathode and anode plates were stainless steel and titanium alloy, respectively.

The system consisted of a CEDI stack, a power supply, and other components such as tanks, pumps, switches, and flow meters (Fig. 1). 60 L feed solution in Reservoir 5 was pumped into the three, separate compartments using diaphragm pumps. The effluent of the dilute compartment was collected in Dilute Reservoir 6 and the effluent of the two concentrate compartments were mixed and collected in Concentrate Reservoir 7. All experiments were performed in constant current mode using one power supply (Shanghai Querli Electrical Equipment Co. Ltd., Shanghai, China). Samples (10 mL) were taken from the dilute and concentrate reservoirs every 0.5 h.

2.2. Experimental protocol

The resin adsorption isotherms of Cs(I), Sr(II), and Co(II) were tested at 30°C using different initial Cs(I), Sr(II), and Co(II) concentrations that ranged from 10–1,000 mg L^{-1}. The mixed resin (0.2 g) was equilibrated with 40 mL of the test solutions; all samples were then agitated on a shaker with 50 rpm for 48 h. The amount of Cs(I), Sr(II), and Co(II) loaded onto the mixed resin q (meq g^{-1}) was calculated using the following equation:

$$q = \frac{C_i - C_e}{m} \times V \quad (1)$$

Table 1
Properties of ion exchange resins

Resin	Resin type	Functional group	Particle size (mm)	Water content (%)	Exchange capacity (eq L^{-1})	Wet density (g L^{-1})
AER	Gel type polystyrene	OH^-	0.58–0.68	54–60	>1.1	690
CER	Gel type polystyrene	H^+	0.30–0.40	45–51	2.0	800

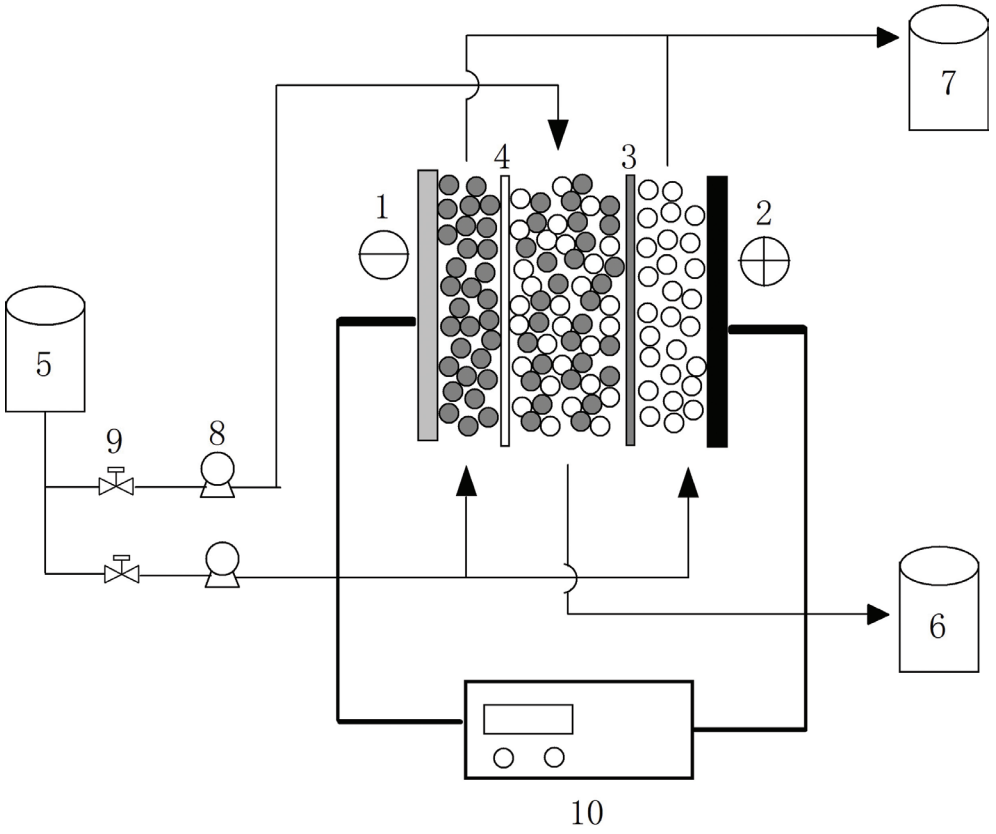

Fig. 1. Electrodeionization unit (○ AER, ● CER, (1) cathode, (2) anode, (3) anion exchange membrane (AEM), (4) cation exchange membrane (CEM), (5) feed solution reservoir, (6) dilute solution reservoir, (7) concentrate solution reservoir, (8) pump, (9) switch, and (10) power supply).

where C_i (meq L^{-1}) and C_e (meq L^{-1}) are the initial and equilibrium concentrations, respectively, of Cs(I), Sr(II), and Co(II) in aqueous solution, V (mL) is the aqueous volume, and m is the mixed resin weight.

Kinetic experiments were performed in a thermostat fitted with a stirrer that rotated at 300 rpm. A total of 0.1 g mixed resin was added to 1 L of solution with an initial concentration of Cs(I), Sr(II), and Co(II) is 2.3, 0.7, and 0.5 mg L^{-1} (the equivalent concentrations of all three ions were 0.017 meq L^{-1}). Samples (5 mL) were taken at set time intervals to measure the concentration of Cs(I), Sr(II), and Co(II).

In order to determine the optimum operation current, the current was changed from 0 to 0.5 A. The corresponding stack voltages and removal efficiency were recorded at a stable condition. The simulated feed water was prepared using $CsNO_3$, $Sr(NO_3)_2$ and $Co(NO_3)_2{\cdot}6H_2O$, and the initial pH of the three solutions were 6.2,5.8 and 6.0, respectively. The initial Cs(I), Sr(II), and Co(II) concentrations were all 0.015 mmol L^{-1}, the feed flow rates to the dilute and concentrate compartments were 80 and 40 mL min^{-1}, respectively.

The characters of CEDI for nuclide removal under the optimum operation current during a long time were investigated. We kept the working current constant at 0.2 A. The initial Cs(I), Sr(II), and Co(II) concentrations were all 0.015 mmol L^{-1}, and the feed flow rates to the dilute and concentrate compartments were 80 and 40 mL min^{-1}, respectively. To minimize any possible adsorption effects, the stack was operated without current prior to any testing until the feed and effluent concentrations were at the same level.

After the end of the experiment, the CER particle in the dilute compartment was randomly selected and cut it into half in order to investigate the migration of nuclide ions in the resin. Changes in resin morphology during the experiments were investigated using scanning electron microscopy (SEM) (SU-8010, HITACHI). As shown in Fig. 2, the distribution of nuclides on the resin profile was investigated using Energy Dispersive Spectrometer (EDS) (SU-8010, HITACHI).

2.3. Analysis

The Cs(I), Sr(II) and Co(II) concentrations were determined using inductively coupled plasma-mass spectroscopy (ICP-MS). All pH values were measured using a Sanxin MP521 Lab pH meter.

The removal efficiency (Re, %) was calculated according to the following equation:

$$\mathrm{Re}(\%) = \left(1 - \frac{C_{t,f}}{C_{0,f}}\right) \times 100 \quad (2)$$

where $C_{t,f}$ is the concentration of Cs(I), Sr(II), and Co(II) at time t in the dilute compartment (mg L^{-1}) and $C_{0,f}$ is the initial Cs(I), Sr(II), and Co(II) concentration in the feed solution (mg L^{-1}).

3. Result and discussion

3.1. CEDI performance on Cs(I), Sr(II) and Co(II) removal

Electrical current is the main driving force for ionic migration in CEDI systems [21–23] and the optimum working current could maximizes ions migration efficiency. Given this, we investigated the effects of electrical current on CEDI performance. The relationship between current and voltage is shown in Fig. 3(a) and the corresponding removal efficiencies of Cs(I), Sr(II), and Co(II) in the dilute compartment at different working currents are shown in Fig. 3(b).

As current increased, both the voltage and the observed removal efficiencies of Cs (I), Sr(II) and Co(II) also increased, but the trends were different. For Cs(I) and Sr(II), at low current (≤0.2 A), the voltage increased linearly with current, which indicate that the current was mainly formed by the migration of nuclide and nitrate ions, so the removal of Cs(I) and Sr(II) increased with the increasing current (Fig. 3(b)).

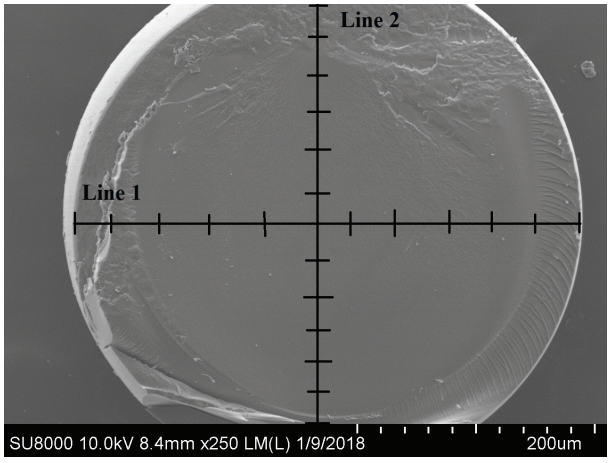

Fig. 2. Distribution of Sampling points on the resin profile.

However, when the current was high (> 0.2 A) the voltage changed hardly with the increase of current, indicating that water dissociation became dominant due to the insufficient number of ions [24,25] and increasing current could not further accelerate nuclide migration and subsequent removal (Fig. 3(b)). The removal efficiencies of Cs(I) and Sr(II) amounted to 99.7% and 98.1% when the current is 0.5 A. For Co(II), the voltage kept increasing at high current (0.2–0.5 A), which was much different with Cs(I) and Sr(II). The Co(II) is easily combining with OH^- which produced by hydrolysis, as given in Eq. (3). The higher the current, the more Co(II) are precipitated from the solution onto the surfaces of resin and membrane. What's more, the deposition hinders ions transport, so the resistance of Co(II) is not significantly reduced like Cs(I) and Sr(II) when the current is high. At a working current of 0.5 A, the removal efficiency of Co(II) amounted to 77.1%.

$$Co^{2+} + 2OH^- = Co(OH)_2\downarrow \quad (3)$$

Fig. 4 shows the effluent concentrations change of Cs(I), Sr(II), and Co(II) in the dilute compartment at the optimum working current, as well as their corresponding pH changes across time. At the start, the effluent concentration was much higher than the feed concentration, but gradually decreased until it reached a stable level. This was accompanied by a simultaneous increase in pH. This phenomenon could be explained as follows: Because the concentration of nuclides in the resin is higher than the solution, there is a significant concentration difference between the resin and solution phases. When an exceeding working current was applied on the CEDI stack (0.2 A), a high potential gradient was existed between the resin and solution phases, which resulted in the hydrolysis at the boundary between these two phases. When the H^+ produced by the hydrolysis reach a certain concentration, the nuclide in the resin is replaced. Therefore, at the start, the effluent concentration was much higher than the feed concentration and the corresponding pH is low. With the gradual decrease in concentration difference between the solid and liquid phases, the hydrolysis became weak and the pH of the effluent gradually increased until it was close to the pH of the feed water.

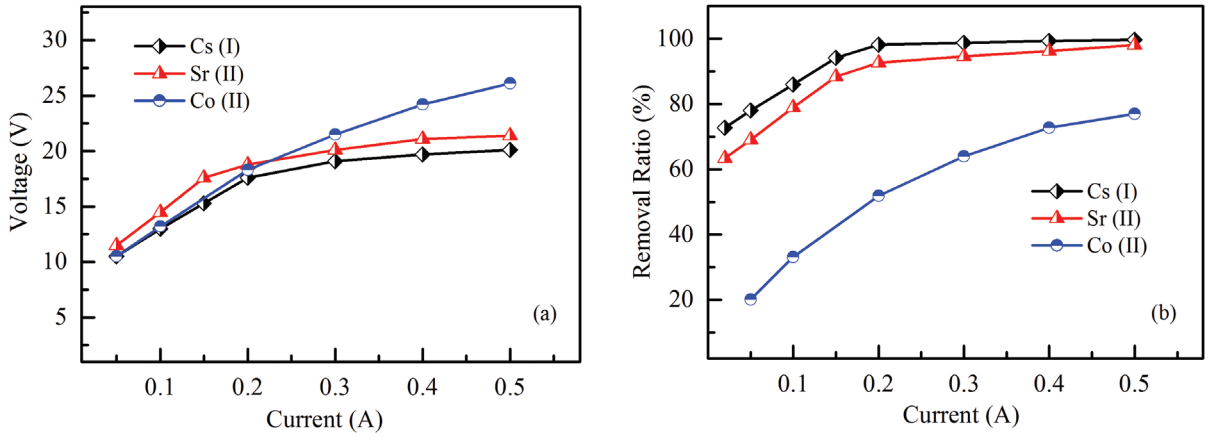

Fig. 3. Variation of voltage (a) and removal ratio and (b) with different working current.

After 7 h of operation, the dilute effluent concentration was stable. The Cs(I), Sr(II), and Co(II) concentrations were 1.58 × 10^{-4} mmol L^{-1}, 5.02 × 10^{-4} mmol L^{-1}, and 9.45 × 10^{-3} mmol L^{-1}, respectively, with corresponding removal efficiencies of 98.2%, 92.7%, and 51.9%. The result can be approved by L.J. Liu research [26], which indicate that the selectivity of CEDI for the three ions is Cs(I) > Sr(II) > Co(II). S.A. Khan [27] treated Sr(II) solution with bentonite, the removal efficiency was 85% when the Sr(II) concentration was 10^{-5} mol L^{-1} and 0.5 g waste was generated when 10 mL solution was treated. When it comes to Cs(I), the removal efficiency was 80% treated by conjugate adsorbents [28]. Compared with the adsorption methods, the CEDI is more effective in the treatment of low level radioactive wastewater and no radioactive waste generated.

The distributions of Cs(I), Sr(II), and Co(II) ions on the resin profile were then analyzed using EDS. For comparison, the resin filled in the normal ion exchange column was also sampled and analyzed. As shown in Fig. 5, we observed that the resin in the ion exchange column had an even ionic distribution. However, the resin in the CEDI stack had differentially distributed Cs(I) and Sr(II) ions according to the electric field. The binding force of the ion and the resin's functional groups affected ionic migration in the resin. This was further demonstrated by the comparable uniform distribution of Co (II) in the resin profile.

3.2. Resin adsorption characteristics of Cs(I), Sr(II) and Co(II)

The aforementioned experimental results showed that the CEDI removal efficiency for Cs(I), Sr(II), and Co(II) under the same conditions followed the following order: Cs(I) > Sr(II) > Co(II). We next sought to determine the isothermic and kinetic parameters of the resin. This was done in order to determine the relationship with the removal behavior in CEDI. To this end, the Langmuir model is often used to fit the resin adsorption process, which allows for a deep analysis of isothermic characteristics [29,30]. Fig. 6 shows a plot of the equilibrium relationship between resin adsorption capacity and the supernatant ion concentration of Cs(I), Sr(II), and Co(II). As shown, the maximum adsorption capacity of the resin for the three ions followed the order Sr(II) > Co(II) > Cs(I).

As shown in Table 2, the theoretical maximum ion exchange adsorption capacity (Q_m) for Sr(II) was 1.77 meq g^{-1}, which was higher than Co(II) (1.55 meq g^{-1}) and Cs(I) (0.81 meq g^{-1}). The result showed that there was no direct relationship between resin adsorption capacity and the performance of CEDI for Cs(I), Sr(II), or Co(II).

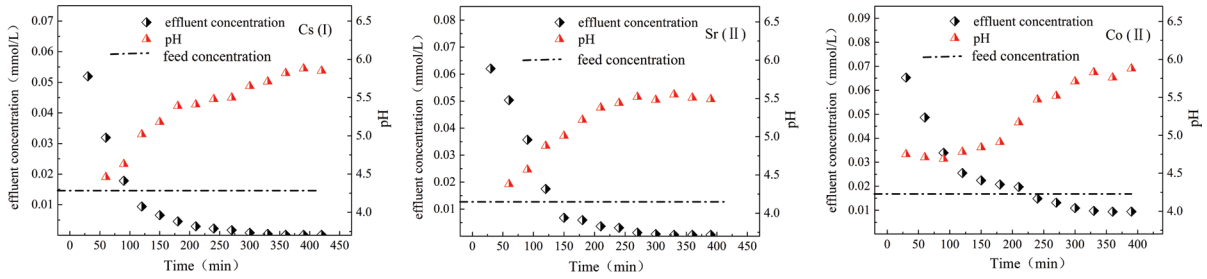

Fig. 4. Variation of effluent concentration and pH value in dilute compartment.

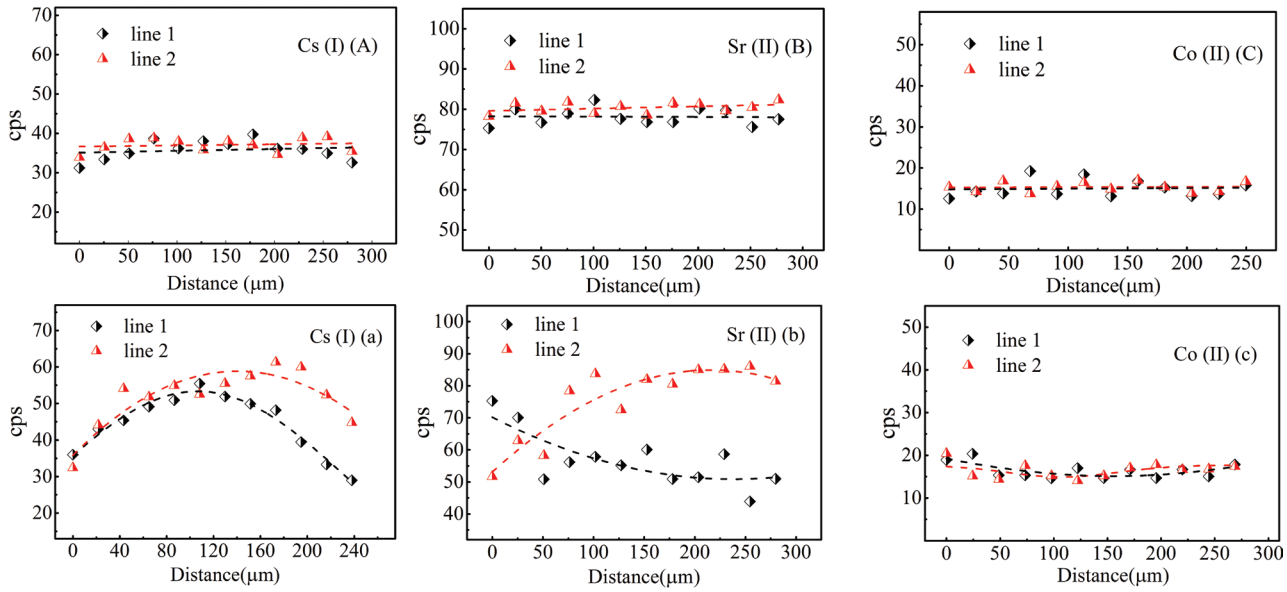

Fig. 5. Distribution of nuclides in the resin profile (A, B, C: resin in the IX bed; a, b, c: resin in CEDI stack).

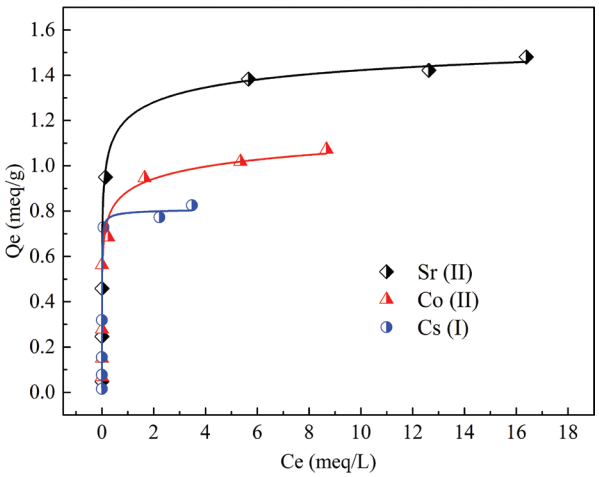

Fig. 6. Adsorption isotherms of Cs(I), Sr(II) and Co(II).

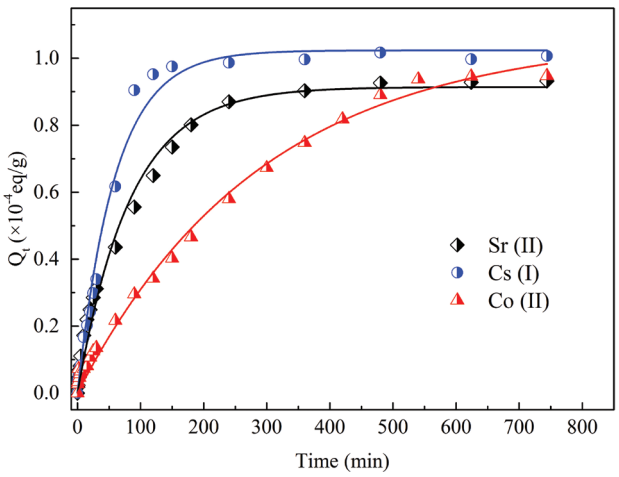

Fig. 7. Adsorption kinetics of Cs(I), Sr(II) and Co(II).

Table 2
Isotherm model fitting results

Model	Parameters	Cs	Sr	Co
Langmuir model	Q_m (meq g^{-1})	0.81	1.77	1.55
	K_L (L mg^{-1})	36.38	2.16	1.33
	R^2	0.997	0.993	0.922

Table 3
Kinetic model fitting results

Model	Parameters	Cs	Sr	Co
Pseudo-second-order	Q_e (×10^{-4} eq g^{-1})	1.16	1.05	1.48
	K_2 (min^{-1})	0.017	0.014	0.0018
	R^2	0.991	0.993	0.998

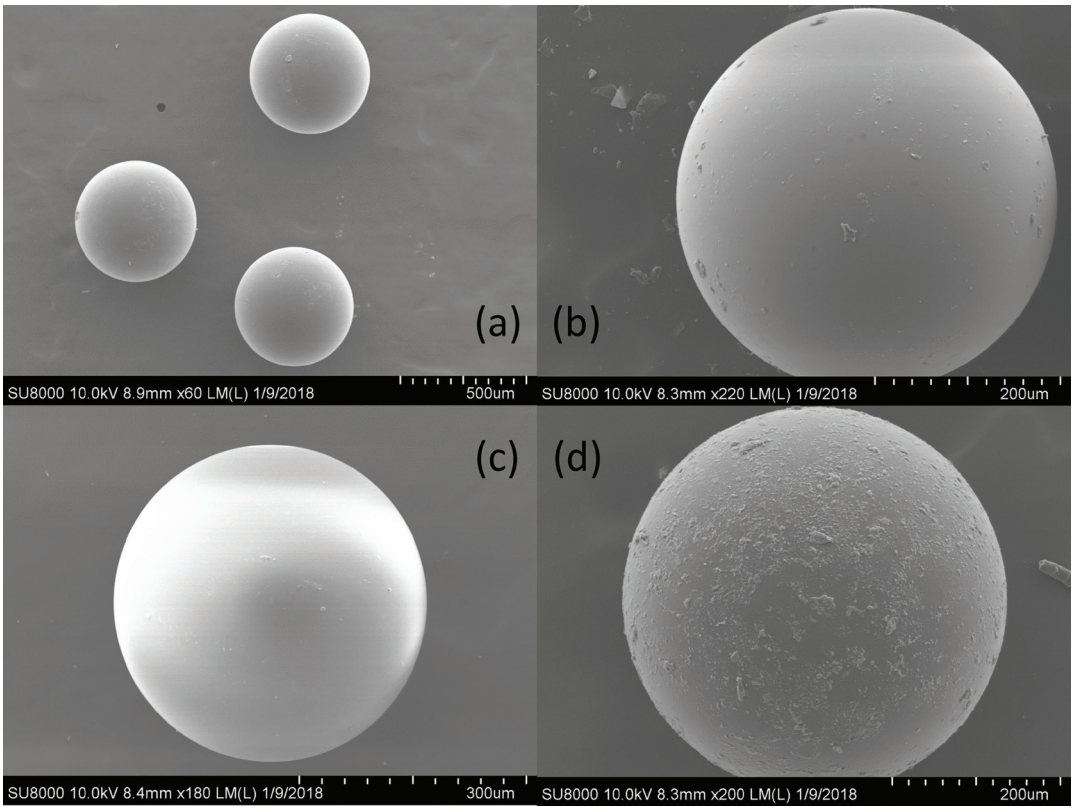

Fig. 8. Analysis of anion exchange resin surface using SEM. (a)virgin, (b) Cs(I), (c) Sr(II), and (d) Co(II).

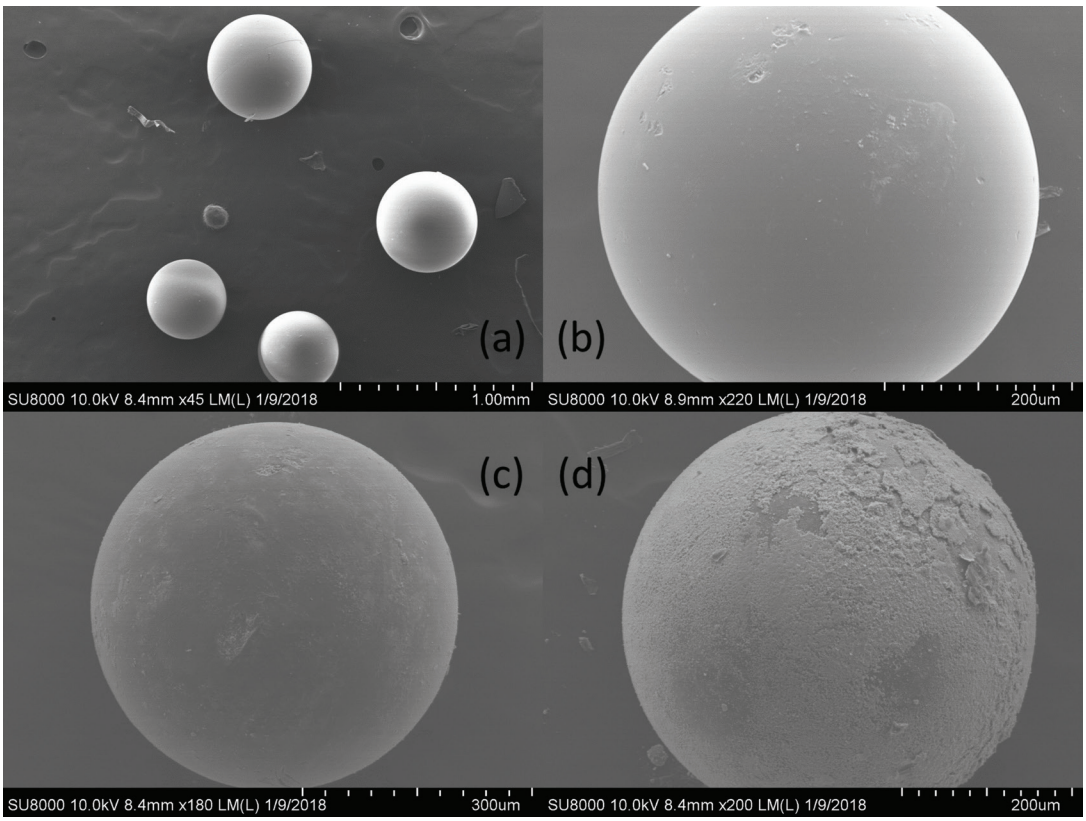

Fig. 9. Analysis of cation exchange resin surface using SEM. (a).virgin, (b).Cs(I), (c).Sr(II), and (d).Co(II).

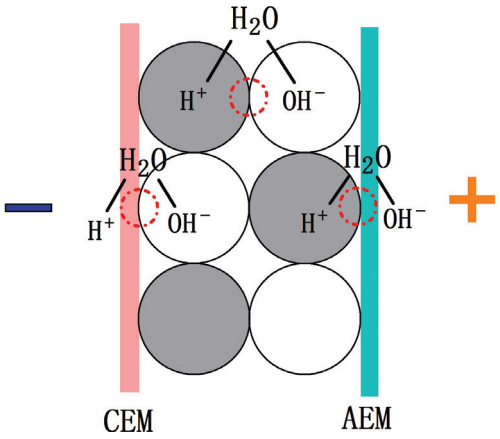

Fig. 10. Schematic hydrolysis illustration of the CEDI system (● : cation exchange resin, ○ : anion exchange resin, CEM: cation exchange membrane, AEM: anion exchange membrane).

Fig. 7 plots the mixed resin adsorption capacity of Cs(I), Sr(II), and Co(II) with reaction time. The adsorption speeds of the mixed resin for Cs(I) and Sr(II) were similar, which were both much higher than Co(II).

Pseudo-second-order kinetic models are the most common model for describing the adsorption kinetics at a liquid-solid interface [31]. The fitting results are shown in Table 3. The reaction rate constant (K_2) of Cs(I) (K_2 = 0.017) was 1.2 times that of Sr(II) (K_2 = 0.014) and 9.4 times that of Co(II) (K_2 = 0.0018).

As shown, the resin adsorption rate for Cs(I), Sr(II), and Co(II) was proportional to the removal efficiency of the CEDI stack to Cs(I), Sr(II), and Co(II). This result indicated that the resin adsorption rate of the ions was an important factor in the removal efficiency of the CEDI stack and this phenomenon was also reported by Jung-Hoon [19].

3.3. Analysis of the resin surface

Figs. 8 and 9 show SEM images of the surface of the anion and cation exchange resin in the dilute compartment. When compared with the virgin cation and anion exchange resins, there was no damage or precipitate formation on the Cs(I)- and Sr(II)-treated resin surfaces. However, the Co(II)-treated resin had slight precipitation on the anion resin surface and a noticeable platelet precipitate was found on the cation resin surface.

Fig. 10 shows the Schematic of hydrolysis in the CEDI system. If the current is too high, the ionic concentration in solution is insufficient and a high potential difference is formed at the bipolar interface (e.g., anion exchange membrane-cation exchange resin, cation exchange membrane-anion exchange resin, cation exchange resin-anion exchange resin). This results in hydrolysis [32]. As a result, the H^+ and OH^- ions migrate in the electric field. When compared with Cs(I) and Sr(II), Co(II) was easier to precipitate with OH^-. This is because Co(II) ions in the cation resin were displaced by H^+ and reacted with OH^-. This resulted in a surface deposit on the cation resin. Due to its proximity to the cation resin, this also resulted in a small amount of precipitate contaminating the surface of anion exchange resin.

4. Conclusions

Here, we tested continuous electrodeionization (CEDI) for its ability to remove trace nuclides such as Cs, Sr, and Co. Our results demonstrated that at a working current of 0.2 A, the removal efficiencies of Cs(I), Sr(II), and Co(II) were 98.2%, 92.7%, and 51.9%., respectively. With an increase in working current to 0.5 A, these values were increased further to 99.7%, 98.1%, and 77.1%, respectively. Cs(I) and Sr(II) actively migrated in the resin and distributed in the resin profile according to the applied electric field. Excessive working current resulted in the hydrolysis and formation of $Co(OH)_2$, which deposited on the surface of the cation exchange resin. Finally, the removal efficiencies for Cs(I), Sr(II), and Co(II) by the CEDI stack were found to be positively related to the adsorption rates of Cs(I), Sr(II), and Co(II) by the resin.

References

[1] F.Z. Li, M. Zhang, X. Zhao, T. Hou, L.J. Liu, Removal of Co^{2+} and Sr^{2+} from a primary coolant by continuous electrodeionization packed with weak base anion exchange resin, Nucl. Technol., 172 (2017) 71–76.

[2] P.C. Gu, S. Zhang, X. Li, X.X. Wang, T. Wen, R. Jehan, A. Alsaedi, T. Hayat, X.K. Wang, Recent advances in layered double hydroxide-based nanomaterials for the removal of radionuclides from aqueous solution, Environ. Pollut., 240 (2018) 493–505.

[3] J. Li, X.X. Wang, G.X. Zhao, C.L. Chen, Z.F. Chai, A. Alsaedi, T. Hayat, X. Wang, Metal-organic framework-based materials: superior adsorbents for the capture of toxic and radioactive metal ions, Chem. Soc. Rev., 47 (2018) 2322–2356.

[4] G.X. Zhao, X.B. Huang, Z.W. Tang, Q.F. Huang, F.L. Niu, X.K. Wang, Polymer-based nanocomposites for heavy metal ions removal from aqueous solution: a review, Polym. Chem., 9 (2018) 3562–3582.

[5] Q. Yang, L. Hou, Y.J. Wang, Progress in study of the low and medium level radioactive liquid waste treatment, Environ. Sci. Manage., 32 (2007) 103–117.

[6] E. Dejean, E. Laktionov, J. Sandeaux, R. Sandeaux, G. Pourcelly, C. Gavach, Electrodeionization with ion-exchange textile for the production of high resistivity water: Influence of the nature of the textile, Desalination, 114 (1997) 165–173.

[7] N. Ghaffour, T.M. Missimer, G.L. Amy, Technical review and evaluation of the economics of water desalination: current and future challenges for better water supply sustainability, Desalination, 309 (2013) 197–207.

[8] T. Itakura, R. SaSai, H. Itoh, Precipitation recovery of boron from wastewater by hydrothermal mineralization, Water. Res., 39 (2005) 2543–2548.

[9] A. Grabowski, G. Zhang, H. Strathmann, G. Eigenberger, The production of high purity water by continuous electrodeionization with bipolar membranes: influence of the anion-exchange membrane permselectivity, J. Membr. Sci., 281 (2006) 297–306.

[10] Ö. Arar, Ü. Yüksel, N. Kabay, M. Yüksel, Application of electrodeionization (EDI) for removal of boron and silica from reverse osmosis (RO) permeate of geothermal water, Desalination, 310 (2013) 25–33.

[11] K.H. Yeon, J.H. Song, S.H. Moon, A study on stack configuration of continuous electrodeionization for removal of heavy metal ions from the primary coolant of a nuclear power plant, Water. Res., 38 (2004) 1911–1921.

[12] M. Tagliabue, A.P. Reverberi, R. Bagatin, Boron removal from water: needs, challenges and perspectives, J. Clean. Prod., 77 (2014) 56–64.

[13] Ö. Arar, Ü. Yüksel, N. Kabay, M. Yüksel, Various applications of electrodeionization (EDI) method for water treatment-A short review, Desalination, 342 (2014) 16–22.

[14] B. Jiang, X. Zhang, X. Zhao, Removal of high level boron in aqueous solutions using continuous electrodeionization (CEDI), Sep. Purif. Technol., 192 (2018) 297–301.

[15] Y.S. Dzyazko, V.N. Belyakov, Purification of a diluted nickel solution containing nickel by a process combining ion exchange and electrodialysis, Desalination, 162 (2004) 179–189.

[16] H.X. Lu, Y.Z. Wang, J.Y. Wang, Removal and recovery of Ni^{2+} from electroplating rinse water using electrodeionization reversal, Desalination, 348 (2014) 74–81.

[17] Y.Q. Xing, X.M. Chen, P.D. Yao, D.H. Wang, Continuous electrodeionization for removal and recovery of Cr(VI) from wastewater, Sep. Purif. Technol., 67 (2009) 123–126.

[18] Ö. Arar, Ü. Yüksel, N. Kabay, Removal of Cu^{2+} ions by a microflow electrodeionization (EDI) system, Desalination, 277 (2011) 296–300.

[19] J.H. Song, K.H. Yeon, S.H. Moon, Transport characteristics of Co^{2+} through an ion exchange textile in a continuous electrodeionization (CEDI) system under electro-regeneration, Sep. Sci. Technol., 39 (2004) 3601–3619.

[20] Y.P. Zhang, L. Wang, S.S. Xuan, Variable effects on electrodeionization for removal of Cs^{+} ions from simulated wastewater, Desalination, 344 (2014) 212–218.

[21] R.V. Pérez, J.I. Mengual, Current-voltage curves for an electrodialysis reversal pilot plant: determination of limiting currents, Desalination, 141 (2001) 23–37.

[22] J.H. Song, K.H. Yeon, S.H. Moon, Effect of current density on ionic transport and water dissociation phenomena in a continuous electrodeionization (CEDI), J. Membr. Sci., 291 (2007) 165–171.

[23] R.Q. Fu, T.W. Xu, W.H. Yang, Z.X. Pan, A new derivation and numerical analysis of current-voltage characteristics for an ion-exchange membrane under limiting current density, Desalination, 173 (2005) 143–155.

[24] L. Fu, J.Y. Wang, Y.L. Su, Removal of low concentrations of hardness ions from aqueous solutions using electrodeionization process, Sep. Purif. Technol., 68 (2009) 390–396.

[25] A. Doyen, C. Roblet, A.L. Gaudet, L. Bazinet, Mathematical sigmoid-model approach for the determination of limiting and over-limiting current density values, J. Membr. Sci., 452 (2014) 453–459.

[26] L.J. Liu, F.Z. Li, X. Zhao, Low-level radioactive wastewater treatment by continuous electrodeionization, J. Tsinghua. Univ. (Sci & Tech)., 48 (2008).1012–1014.

[27] S.A. Khan, Sorption of the long-lived radionuclides cesium-134, strontium-85 and cobalt-60 on bentonite, J. Radioanal. Nucl Chem., 258 (2003) 3–6.

[28] M.R. Awual, S. Suzuki, T. Taguchi, H. Shiwaku, Y. Okamoto, T. Yaita, Radioactive cesium removal from nuclear wastewater by novel inorganic and conjugate adsorbents, Chem. Eng. J., 242 (2014) 127–135.

[29] E. Korngold, N. Belayev, L. Aronov, Removal of chromates from drinking water by anion exchangers, Sep. Purif. Technol., 33 (2003) 179–187.

[30] X. Qu, M. Tian, B.Q. Liao, A.C. Chen, Enhanced electrochemical treatment of phenolic pollutants by an effective adsorption and release process, Electrochim. Acta, 55 (2010) 5367–5374.

[31] S. Chowdhury, P. Saha, Adsorption kinetic modeling of safranin onto rice husk biomatrix using pseudo-first-order and pseudo-second-order kinetic models: comparison of Linear and Non-linear methods, CLEAN-Soil. Air. Water., 39 (2011) 274–282.

[32] L. Dohyeon, L.J. Young, K. Yekyung, Investigation of the performance determinants in the treatment of arsenic-contaminated water by continuous electrodeionization, Sep. Purif. Technol., 179 (2017) 381–392.